

View Article Online
View Journal

Cite this: DOI: 10.1039/c3cc00133d

DOI: 10.1039/c3cc00133d

www.rsc.org/chemcomm

Preserved high first triplet energy levels and improved electrical properties of two donor–acceptor type carbazole–phosphine oxide hosts were achieved through short-axis substitution to realize efficient PHOLEDs with extremely low driving voltages of 2.6 V for onset and <3.2 V at 100 cd m^{-2} .

Recently, low-voltage-driving blue phosphorescent organic light-emitting diodes (PHOLEDs) have become attractive due to their potential applications in portable devices.¹ This requires the host materials to have both high first triplet energy level (T_1) (> 2.8 eV) and good carrier injecting/transporting ability. One of the main strategies is constructing ambipolar systems with high T_1 through blocking the interplays between donors (D) and acceptors (A) by involving spacers or insulating linkages,² which either somewhat decrease T_1 or weaken carrier injection/transportation. In this case, some electrically active insulating linkages, such as phosphine oxide (PO), are involved in hosts for improving carrier injection and transportation while preserving high T_1 .³ However, it is still a big challenge to control the optoelectronic properties of the PO involved D–A type hosts. At the same time as decreasing the energy levels of the LUMOs, the strong electron-withdrawing effect of the P=O group along the long axis of the D-type chromophores, such as carbazole, also remarkably reduces the energy levels of the HOMOs. As a result, the first singlet excited energy levels (S_1) are unchanged or even enlarged. In this sense, the improvement of electron injection by PO groups is at the cost of weakening the hole injection of the chromophores, like the situation of carbazole–phosphine oxide hybrids.⁴ Our group have reported several high-efficiency PO hosts based on short-axis linkage,⁵ multi-insulating linkage⁶ or indirect linkage.⁷ It was shown that the short-axis

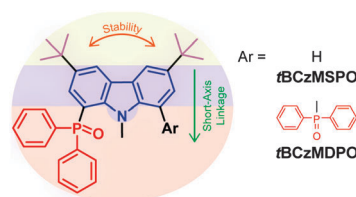
linkage can amplify the molecular polarization. Recently, we further demonstrated ultra-low-voltage driving PHOLEDs of two short-axis substituted dibenzothiophene-PO hosts, in which the negative influence on HOMOs by PO groups was suppressed by the long-range backing bonding effect between S and P atoms.^{5d} Nevertheless, the effect of short-axis substitution on optoelectronic properties of D-A systems is still not clear.

In this contribution, we report the controllable modulation of the optoelectronic properties of two carbazole–phosphine oxide hybrids for low-voltage driving electrophosphorescence, namely 3,6-di-*tert*-butyl-1-(diphenylphosphoryl)-9-methyl-9*H*-carbazole (**tBCzMSPO**) and 3,6-di-*tert*-butyl-1,8-bis(diphenylphosphoryl)-9-methyl-9*H*-carbazole (**tBCzMDPO**) with the collective name of **tBCzMxPO**, in which electron-transporting diphenylphosphine oxide (DPPO) groups are bonded at the 1,8-position of carbazolyl to form the local unsymmetrical D–A configuration (Scheme 1 and Scheme S1†). Accompanied by the high T_1 , the hole injecting ability of carbazolyl might be preserved to a great extent for achieving the ambipolar characteristics of **tBCzMxPO**. The investigation indicated their T_1 of 2.98 eV and suppressed influence of DPPO on their HOMOs. As a result, the controllable tuning of optoelectronic properties by short-axis linkage was successfully realized by remarkably improving electron injecting/transporting ability with reduced influence on other photoelectronic properties. Efficient blue PHOLEDs based on **tBCzMxPO** were realized with driving voltages of only 2.6 V for onset and <3.2 V at 100 cd m^{−2}, which were among the best results of carbazole-type high-energy-gap host materials. Significantly, this work establishes a solid example for controlling photoelectronic properties of

^a Key Laboratory of Functional Inorganic Material Chemistry, School of Chemistry and Materials, Heilongjiang University, Ministry of Education, Harbin 150080, P. R. China. E-mail: hxxu@hlju.edu.cn; Fax: +86 451 86608042

^b State Key Laboratory on Integrated Optoelectronics, College of Electronics Science and Engineering, Jilin University, 2699 Qianjin Street, Changchun 130012, P. R. China. E-mail: zhao_yi@jlu.edu.cn

† Electronic supplementary information (ESI) available: Experimental details, thermal properties, absorption and PL spectra, CV curves and EL performance of the devices. See DOI: 10.1039/c3cc00133d



Scheme 1 Design strategy and molecular structures of **tBCzMxPO**.

D–A type hosts by careful management of molecular configurations and intramolecular interplays.

The temperature of decomposition (T_d , at weight loss of 5%) of **tBCzMSPO** is 323 °C. An extra DPPO in **tBCzMDPO** results in a higher T_d of 394 °C, which should be ascribed to the reduced molecular volatility (Fig. S1†). The melting point (T_m) of **tBCzMSPO** is 206 °C, accompanied by a rather high temperature of glass transition (T_g) of 175 °C, which indicates its improved phase stability. **tBCzMDPO** has a much higher T_m of 340 °C even though no distinct T_g was observed. The high quality of vacuum evaporated thin films of **tBCzMxPO** was demonstrated by AFM and SEM images with the limited roughness of about 0.2 nm (Fig. S2†). The remarkably enhanced thermal stability and film formability of **tBCzMxPO** is due to the compact and rigid configuration by short-axis substitution, which is crucial for the improvement of device interfaces and stability.

The optical properties of **tBCzMxPO** in dilute solutions (10^{-6} mol L $^{-1}$ in dichloromethane) are nearly the same. Their absorption spectra consist of four bands at about 350 (n \rightarrow π^* transition of carbazoyl), 300 (n \rightarrow π^* transition from carbazoyl to DPPO), 250 ($\pi \rightarrow \pi^*$ transition of carbazoyl) and 230 nm ($\pi \rightarrow \pi^*$ transition of DPPO) (Fig. 1 and Table S1†). The larger absorption cross section of **tBCzMDPO** induces its larger extinction coefficient, especially for the DPPO-involved transitions. The fluorescent (FL) emissions of **tBCzMxPO** in solution at room temperature are also similar, with peaks at 390 nm, accompanied by almost equal lifetimes of ~ 5 ns (Fig. S3†). Nevertheless, S_1 of **tBCzMDPO** is 3.26 eV, estimated according to the absorption edge, which is about 0.1 and 0.18 eV smaller than those of **tBCzMSPO** and 3,6-di-*tert*-butyl-9-methyl-carbazole (**tBCzM**) (Fig. S4†), respectively. This indicates the accumulated polarization by short-axis substituted DPPOs. The similar emissions of **tBCzMxPO** in solvents with different polarities further reveal the suppressed intramolecular charge transfer by short-axis linkage (Fig. S6†). T_1 s of **tBCzMxPO** are estimated according to 0–0 transitions of their time-resolved phosphorescent (PH) spectra at 77 K in CH $_2$ Cl $_2$ glasses, which are 2.98 eV, the same as that of **tBCzM**. Thus, preserving T_1 and polarizing molecules are simultaneously realized in **tBCzMxPO** by short-axis substitution. The energy gaps between S_1 and T_1 (ΔE_{ST}) of **tBCzMSPO** and **tBCzMDPO** are only 0.38 and 0.28 eV, respectively, which are among the smallest results reported so far and imply the improved carrier injecting ability.

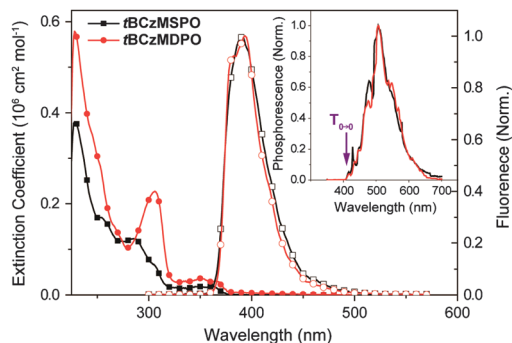


Fig. 1 Absorption and emission spectra of **tBCzMxPO** in dilute CH $_2$ Cl $_2$.

The nature of the modulated optical properties of **tBCzMxPO** was investigated by DFT calculation (Fig. 2). The configurations and frontier molecular orbitals (FMOs) of 3,6-substituted analogues **3tBCzMSPO** and **36CzMDPO**, as well as **tBCzM**, were also simulated for comparison. The HOMOs and LUMOs of all of the compounds are mainly located on carbazoyls. The methyls are also involved in the HOMOs due to the super-conjugation effect. The incorporation of DPPOs at 3,6-positions in **3tBCzMSPO** and **36CzMDPO** induces a significant reduction of LUMO energy levels (0.247 and 0.243 eV, respectively, while in **tBCzMxPO** the first and second DPPOs result in reductions of LUMOs of 0.300 and 0.136 eV, respectively. Thus, **tBCzMxPO** have LUMO energy levels comparable with their 3,6-substituted analogues. However, compared with that of **tBCzM**, HOMOs of **3tBCzMSPO** and **36CzMDPO** are even more remarkably reduced, by 0.327 and 0.635 eV, respectively. Therefore, the HOMO–LUMO energy gaps of these 3,6-substituted analogues are even larger than that of **tBCzM**. Contrarily, for **tBCzMxPO** the negative effect of DPPO on the HOMO is effectively suppressed such that the first and second DPPOs only result in slight reductions of HOMOs of 0.136 and 0.082 eV, respectively. As a result, their HOMO–LUMO energy gaps are successfully decreased by 0.164 and 0.218 eV, respectively. This is in accord with the experimental data measured by cyclic voltammetry that the HOMO energy levels were 5.85, 5.99 and 6.13 eV for **tBCzM**, **tBCzMSPO** and **tBCzMDPO**, respectively (Fig. S7†). The J – V characteristics of the nominal single-carrier transporting devices based on **tBCzMSPO** indicated that its hole-only current density (J) was much larger than its electron-only J , which revealed the suppressed negative influence of short-axis substituted DPPO on hole transportation of carbazoyl (Fig. S8†). However, the hole-only J and electron-only J of **tBCzMDPO** are comparable, which indicated the remarkable contribution of DPPO to electron transportation and the limited embedding effect of DPPOs on carbazoyl. Therefore, the electron injecting/transporting ability of **tBCzMxPO** is dramatically improved with controllable influence on their hole injecting/transporting ability, which contrasts sharply with their long-axis substituted analogues.⁴

The high T_1 and modified electrical properties of **tBCzMxPO** encouraged us to investigate their performance as hosts in blue-emitting PHOLEDs **BA–BD** with configuration of ITO|MoO $_x$

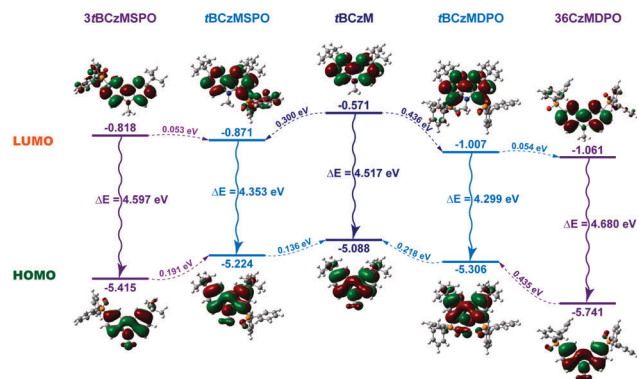


Fig. 2 DFT calculation results of **tBCzMxPO**, **tBCzM** and 3,6-substituted analogues.

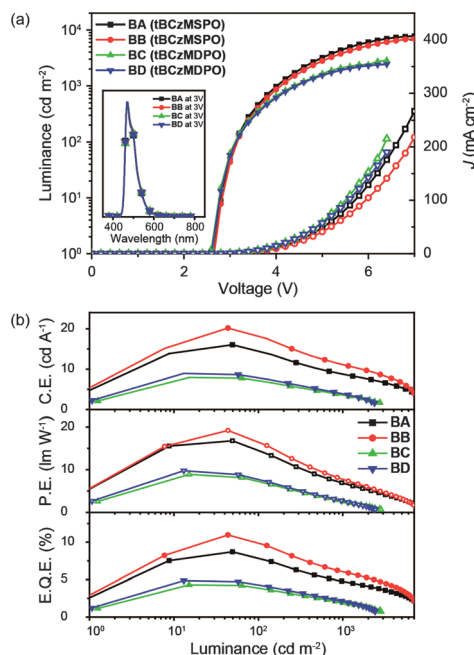


Fig. 3 B–J–V curves (a) and efficiency curves (b) of blue-emitting PHOLEDs based on **tBCzMxPO**.

(2 nm)|*m*-MTDATA:MoO_x (15%, 30 nm)|*m*-MTDATA (10 nm)|Ir(ppz)₃ (10 nm)|**tBCzMxPO**:10% Flrpic (10 nm)|3TPYMB (*y* nm)|Bphen (40 – *y* nm)|Cs₂CO₃ (1 nm)|Al (*y* = 0 for **BA** and **BC**; *y* = 10 for **BB** and **BD**) (Fig. 3 and Scheme S2†). The turn-on voltages of these devices were only 2.6 V, which is much lower than those of devices based on other carbazole derivatives.⁴ For **BA** and **BB**, practical luminance of 100 and 1000 cd m^{−2} for display and lighting were achieved at rather low voltages of <3.2 and ~4 V, respectively. **BA** showed the maximum efficiencies of 16.0 cd A^{−1} for current efficiency (CE), 16.8 lm W^{−1} for power efficiency (PE) and 8.7% for external quantum efficiency (EQE). The bigger PE than CE was due to its low driving voltages. At 100 cd m^{−2}, the efficiency roll-offs were only 15% for CE, 20% for PE and 15% for EQE. The involvement of an exciton-blocking 3TPYMB layer in **BB** further improve the maximum efficiencies to 20.2 cd A^{−1}, 19.2 lm W^{−1} and 11.0% with further reduced corresponding roll-offs at 100 cd m^{−2} as 13, 18 and 13%. It is noticed that at high driving voltages, *J* of **BC** and **BD** was slightly higher than that of **BA** and **BB**, which is in accord with the results of DFT calculation and CV analysis. Considering the same optical properties of **tBCzMxPO**, the lower luminance at high voltages and reduced efficiency of **BC** and **BD** should be attributed to the narrow exciton composition zone due to the too strong electron transporting ability of **tBCzMDPO**, which worsened the concentration quenching at high voltages. The localization of exciton composition at the interface between Ir(ppz)₃ and EMLs was further demonstrated by the similar efficiencies of **BC** and **BD**. The green- and yellow-emitting PHOLEDs of **tBCzMSPO** were also fabricated with similar configuration except for the dopants (Ir(ppy)₃, 6% and PO-01, 6%) (Fig. S9†). The extremely

low driving voltages of 2.6 V for onset, <3.0 V at 100 cm^{−2} and <3.4 V at 1000 cd m^{−2} were also realized as well as high efficiencies (Table S2†).

In summary, this work successfully demonstrated the controllable modulation of optoelectronic properties of two D–A type hosts **tBCzMSPO** and **tBCzMDPO** on the basis of short-axis linkage. The modified electrical performance and preserved *T*₁ of **tBCzMSPO** endowed its efficient PHOLEDs with extremely low driving voltages of 2.6 V for onset and about 3.0 V at 100 cm^{−2} for portable display.

W.Y., Z.S.Z. and C.H. contributed equally to this work. This project was financially supported by the National Key Basic Research and Development Program of China (2010CB327701), NSFC (50903028, 61176020 and 61275033), New Century Talents Supporting Program of MOE, Key Project of MOE (212039), New Century Talents Developing Program of Heilongjiang Province (1252-NCET-005), Education Bureau of Heilongjiang Province (10td03), and the Supporting Program of Highlevel Talents of HLJU (2010hdt08).

Notes and references

- (a) M. A. Baldo, D. F. O'Brien, Y. You, A. Shoustikov, S. Sibley, M. E. Thompson and S. R. Forrest, *Nature*, 1998, **395**, 151; (b) S. J. Su, H. Sasabe, Y. J. Pu, K. Nakayama and J. Kido, *Adv. Mater.*, 2010, **22**, 3311; (c) R.-F. Chen, G.-H. Xie, Y. Zhao, S.-L. Zhang, J. Yin, S.-Y. Liu and W. Huang, *Org. Electron.*, 2011, **12**, 1619; (d) H. Sasabe, N. Toyota, H. Nakanishi, T. Ishizaka, Y.-J. Pu and J. Kido, *Adv. Mater.*, 2012, **24**, 3212; (e) Y. J. Cho and J. Y. Lee, *Adv. Mater.*, 2011, **23**, 4568.
- (a) K. S. Yook and J. Y. Lee, *Adv. Mater.*, 2012, **24**, 3169; (b) S. Gong, Q. Fu, W. Zeng, C. Zhong, C. Yang, D. Ma and J. Qin, *Chem. Mater.*, 2012, **24**, 3120; (c) L. Xiao, Z. Chen, B. Qu, J. Luo, S. Kong, Q. Gong and J. Kido, *Adv. Mater.*, 2011, **23**, 926; (d) Y. Tao, C. Yang and J. Qin, *Chem. Soc. Rev.*, 2011, **40**, 2943; (e) Y.-M. Chen, W.-Y. Hung, H.-W. You, A. Chaskar, H.-C. Ting, H.-F. Chen, K.-T. Wong and Y.-H. Liu, *J. Mater. Chem.*, 2011, **21**, 14971.
- (a) A. B. Padmaperuma, L. S. Sapochak and P. E. Burrows, *Chem. Mater.*, 2006, **18**, 2389; (b) P. A. Vecchi, A. B. Padmaperuma, H. Qiao, L. S. Sapochak and P. E. Burrows, *Org. Lett.*, 2006, **8**, 4211; (c) H. Liu, G. Cheng, D. Hu, F. Shen, Y. Lv, G. Sun, B. Yang, P. Lu and Y. Ma, *Adv. Funct. Mater.*, 2012, **22**, 2830; (d) N. Lin, J. Qiao, L. Duan, H. Li, L. Wang and Y. Qiu, *J. Phys. Chem. C*, 2012, **116**, 19451; (e) J. Zhao, G.-H. Xie, C.-R. Yin, L.-H. Xie, C.-M. Han, R.-F. Chen, H. Xu, M.-D. Yi, Z.-P. Deng, S.-F. Chen, Y. Zhao, S.-Y. Liu and W. Huang, *Chem. Mater.*, 2011, **23**, 5331; (f) S. O. Jeon, S. E. Jang, H. S. Son and J. Y. Lee, *Adv. Mater.*, 2011, **23**, 1436; (g) H.-H. Chou and C.-H. Cheng, *Adv. Mater.*, 2010, **22**, 2468; (h) F.-M. Hsu, C.-H. Chien, C.-F. Shu, C.-H. Lai, C.-C. Hsieh, K.-W. Wang and P.-T. Chou, *Adv. Funct. Mater.*, 2009, **19**, 2834.
- S. O. Jeon, K. S. Yook, C. W. Joo and J. Y. Lee, *Adv. Funct. Mater.*, 2009, **19**, 3644.
- (a) C. Han, G. Xie, H. Xu, Z. Zhang, L. Xie, Y. Zhao, S. Liu and W. Huang, *Adv. Mater.*, 2011, **23**, 2491; (b) C. Han, G. Xie, H. Xu, Z. Zhang, D. Yu, Y. Zhao, P. Yan, Z. Deng and S. Liu, *Chem.-Eur. J.*, 2011, **17**, 445; (c) C. Han, Z. Zhang, H. Xu, J. Li, G. Xie, R. Chen, Y. Zhao and W. Huang, *Angew. Chem., Int. Ed.*, 2012, **51**, 10104; (d) C. Han, Z. Zhang, H. Xu, S. Yue, J. Li, P. Yan, Z. Deng, Y. Zhao, P. Yan and S. Liu, *J. Am. Chem. Soc.*, 2012, **134**, 19179.
- (a) C. Han, Y. Zhao, H. Xu, J. Chen, Z. Deng, D. Ma, Q. Li and P. Yan, *Chem.-Eur. J.*, 2011, **17**, 5800; (b) C. Han, Z. Zhang, H. Xu, G. Xie, J. Li, Y. Zhao, Z. Deng, S. Liu and P. Yan, *Chem.-Eur. J.*, 2013, **19**, 141.
- (a) D. Yu, Y. Zhao, H. Xu, C. Han, D. Ma, Z. Deng, S. Gao and P. Yan, *Chem.-Eur. J.*, 2011, **17**, 2592; (b) D. Yu, F. Zhao, C. Han, H. Xu, J. Li, Z. Zhang, Z. Deng, D. Ma and P. Yan, *Adv. Mater.*, 2012, **24**, 509.